Applied Surface Science 346 (2015) 388–393

Contents lists available at ScienceDirect

Applied Surface Science

journal homepage: www.elsevier.com/locate/apsusc

Anisotropy of synthetic diamond in catalytic etching using iron powder

Junsha Wang[a,b], Long Wan[a,*], Jing Chen[a], Jiwang Yan[b]

[a] College of Materials Science and Engineering, Hunan University, Hunan 410082, PR China
[b] Department of Mechanical Engineering, Keio University, Yokohama 223-8522, Japan

ARTICLE INFO

Article history:
Received 15 October 2014
Received in revised form 5 March 2015
Accepted 3 April 2015
Available online 11 April 2015

Keywords:
Synthetic diamond crystallite
Catalytic etching
Iron
Temperature
Crystal plane

ABSTRACT

This paper demonstrated a novel technique for catalytic etching of synthetic diamond crystallites using iron (Fe) powder without flowing gas. The effect of temperature on the etching behaviour on different crystal planes of diamond was investigated. The surface morphology and surface roughness of the processed diamond were examined by scanning electron microscope (SEM) and laser-probe surface profiling. In addition, the material composition of the Fe-treated diamond was characterized using micro-Raman spectroscopy and the distribution of chemical elements and structural changes on Fe-loaded diamond surfaces were analyzed by energy dispersive X-ray spectroscopy (EDS) and X-ray diffraction (XRD), respectively. Results showed that at the same temperature the {1 0 0} plane was etched faster than the {1 1 1} plane, and that the etching rate of both {1 0 0} and {1 1 1} plane increased with temperature. The etch pits on {1 0 0} plane were reversed pyramid with flat {1 1 1} walls, while the etch holes on {1 1 1} plane were characterized with flat bottom. It was also demonstrated that graphitization of diamond and subsequent carbon diffusion in molten iron were two main factors resulting in the removal of carbon from the diamond surface.

1. Introduction

Owing to the exceptional mechanical properties, such as high hardness, high wear resistance and its ability to form extremely sharp cutting edges, diamond has been widely used in precision manufacturing industries [1,2]. To improve the functionality of diamond and to increase its applicability to other related fields, extensive research is being done concerning surface modification of diamond. Extant literature on gasification of carbon suggests that in the presence of hydrogen, graphite will gasify into methane and furthermore, transition metals can accelerate the gasification process significantly [3,4]. Studies on gasification of graphite have also showed the formation of etch channels [5] and tunnels [6], which led to the subsequent development of the process known as metal catalytic hydrogenation of diamond.

The earliest efforts concerning diamond patterning using Fe, Ni and Pt films under hydrogen atmosphere led to a lore of metallic iron being the most active catalyst [7]. Afterwards, Chepurov et al. [8–10] performed etching of synthetic diamond crystallites with iron particles loaded in a hydrogen atmosphere to investigate the anisotropic etching patterns on different crystal planes. Their results showed that the irregular channels with flat bottom appeared on the {1 1 1} face, while linear cavities were formed on the {1 0 0} and the {1 1 0} faces. It was also observed that etching on the {1 1 1} plane of synthetic diamond proceeded in tangential direction whereas in natural diamond etching occurred preferentially in a normal direction [11]. However, when synthetic diamond crystallites were etched using iron particles which were reduced from ferric chloride by hydrogen gas, etching along the tangential direction was completely absent. Instead, the iron particles penetrated deeper into the volume of diamond leading to the formation of nano pits and tunnels [12]. Most surprisingly, the anisotropy of etching was found non-existent as well [13].

Since then, series of attempts have been made to optimize the etching process by varying the preparative methods and the annealing atmosphere of metal-diamond mixture. An impregnation method was developed to load the ferric nitrate on diamond crystallites and the effect of crystal plane on the etching behaviour at 900 °C in a flowing gas mixture of H_2 (10%) + N_2 (90%) was investigated [14]. Results showed that nanochannels with flat walls perpendicular to the surface were formed on the {1 1 1} plane, while an array of etch pits on the {1 0 0} plane reflecting the atomic arrangements on the corresponding surface was identified. Additionally, the formation of iron carbide-like particles during the iron

* Corresponding author. Tel.: +86 731 88823540; fax: +86 731 88823540.
E-mail addresses: wanlong1799@163.com, wanlong1799@aliyun.com (L. Wan).

http://dx.doi.org/10.1016/j.apsusc.2015.04.022
0169-4332/

etching process was also postulated. More recently, a simple technique to etch the diamond by self-assembled metals under mixed hydrogen and nitrogen atmosphere was proposed [15]. According to this method, thin iron layers were vacuum evaporated on the {1 0 0}-oriented diamond film and different etching temperatures and holding times were compared. Observations at 800 °C indicated that except the edge part, no etching occurred. Further heating at 900 °C resulted in the formation of some vacant etch pits and channels because Fe particles slipped out of the pits. Under the same conditions, an increase in annealing time led to the appearance of obvious etch pits and channels with four flat walls.

Hence, the above literatures suggest that although a modicum of success has been attained in etching diamond surface using iron but the process requires the use of hydrogen as a flowing gas. Using hydrogen gas increases processing cost and may cause safety problems. From this meaning, it is necessary to develop research on diamond etching without using flowing hydrogen gas. However, up to date, very little has been done to etch diamond without flowing hydrogen. The primary objective of this study was to eliminate the need of a flowing gas while etching diamond using iron. Most importantly, there is no systematic study evident in the literature which would show the dependence of temperature on the anisotropic etching behaviour of synthetic diamond which partly motivated this study as well. Accordingly, the methodology of the experiments and the observations gathered from the experiments are being discussed in this paper.

2. Experimental details

This experimental study made use of diamond crystallites (LD 240 from Henan Liliang New Material Co., Ltd.) with average diameter of 0.5 mm and iron particles with size distribution of 2–10 μm. As for the process of sample preparation, diamond and iron powder in a weight ratio of 1–13 were mixed thoroughly using stirring rod. In order to ensure a close contact between the diamond crystallites and iron powder, the mixture was gently pressed by slide glasses. Subsequently, samples were wrapped with the graphite paper to avoid the influence of oxygen from air on the etching process. Then, samples were placed in the graphite crucible full of carbon black powder, which was set in a closed ceramic crucible with carbon black. Finally the ceramic crucible with sample contained was moved into the muffle furnace. Heating rate from room temperature to 600 °C was set at 3 °C/min which changed to 2 °C/min until 750 °C. In order to ensure the close contact between the surfaces of melt iron and diamond, the heating rate was then slowed to 1.5 °C/min. After the temperature reached the objective etching temperature, it was retained for one hour. After the catalytic treatment, the annealed bulk samples were rinsed in aqua regia ($HCl:HNO_3 = 3:1$) to remove the excess iron particles and the specimens were labelled as Fe-treated diamond. The surfaces of the Fe-treated diamond were measured using a laser probe and maximum Peak-to-Valley (P–V) value was used as an index for characterizing the extent of etching. The surface morphology and distribution of chemical elements of the specimens were done using scanning electron microscopy (SEM) and energy dispersive X-ray spectrometer (EDX) while the chemical composition was characterized by X-ray diffraction (XRD).

3. Results

3.1. Surface morphology of diamond crystallites

Fig. 1 shows the morphology of pristine crystallites of synthetic diamond. The as-received synthetic diamond crystallites had cubo-octahedral structure i.e. eight surfaces oriented on the {1 1 1} plane and six surfaces oriented on the {1 0 0} plane while

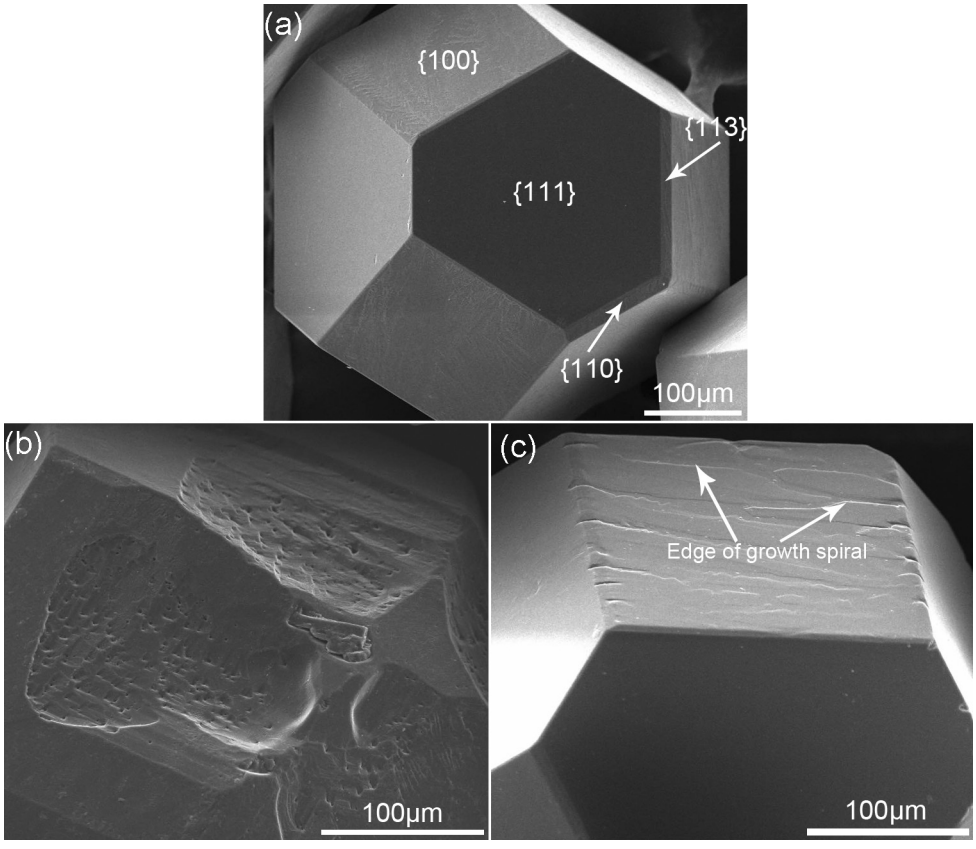

Fig. 1. Morphology of pristine synthetic diamond crystallites: (a) well-grown diamond crystallite; (b) and (c) growth defects on diamond surfaces.

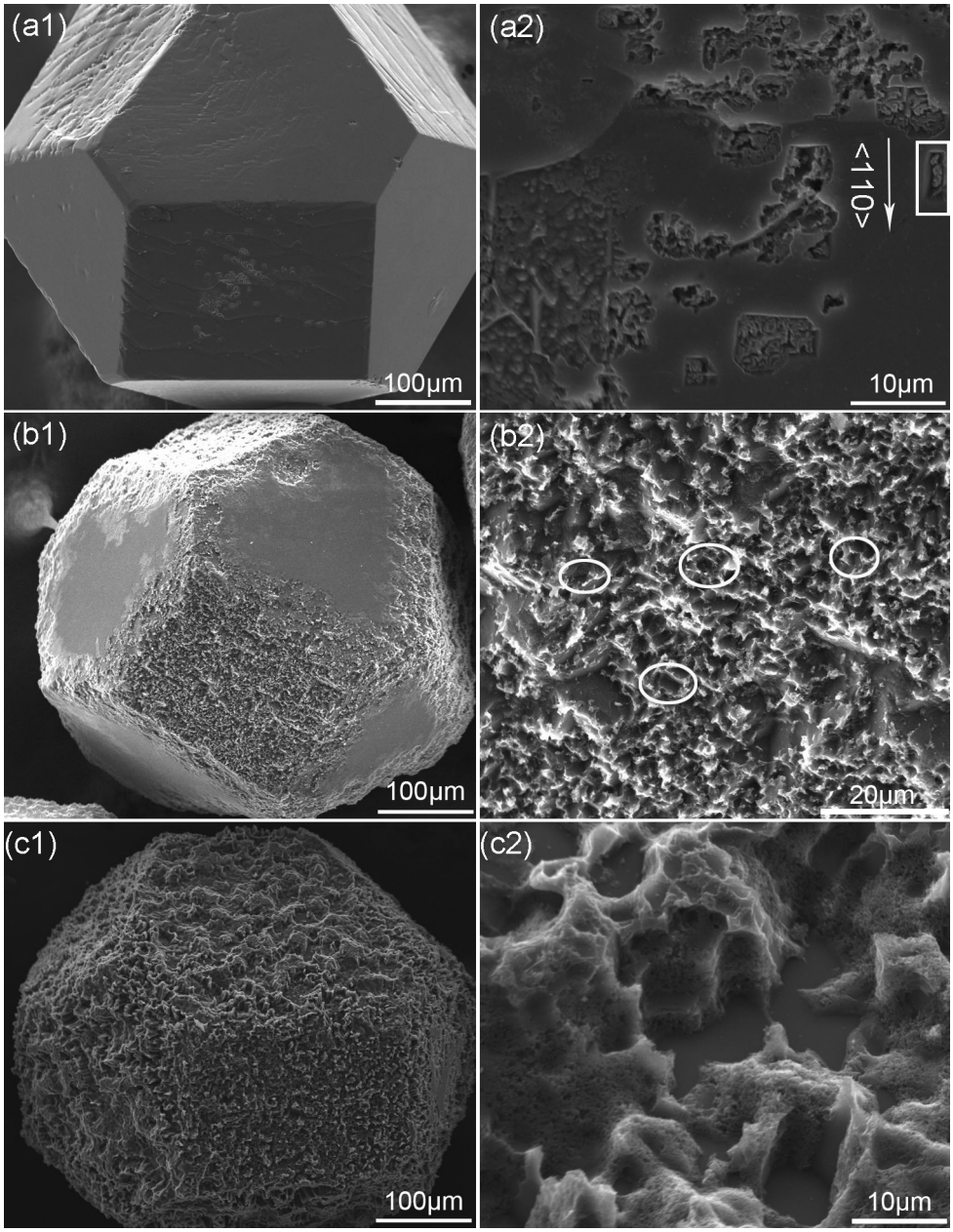

Fig. 2. SEM images of Fe-treated diamond crystallites annealed at different temperatures: (a1), (a2): 850 °C; (b1), (b2): 900 °C; (c1), (c2): 950 °C.

the secondary faces of {1 1 3} and {1 1 0} planes were also visible. Although growth defects, e.g. structural imperfection and growth steps were inevitably present on few diamond crystallites, no obvious etch pits or channels were observed.

SEM images of Fe-treated diamond crystallites at different temperatures are shown in Fig. 2. The observations concerning the etching behaviour on different planes of diamond at different temperatures have been summarized in Table 1. Generally speaking, it was observed that the {1 0 0} plane is easier to be etched in comparison with the {1 1 1} plane at the same etching temperature while the extent of etching on both {1 0 0} and the {1 1 1} plane increases with the etching temperature.

3.2. The extent of etching on diamond surface

In order to quantify the extent of etching on various crystal planes of diamond, a laser probe was used to measure the peak-to-valley value (P–V value) on the etched diamond surfaces. To ensure repeatability in the reported results, at least twenty measurements were made on each type of etched surface. The measured results were plotted and compared on a histogram shown in Fig. 3. It can be seen that the P–V value of {1 1 1} plane increases gradually with the etching temperature, while that of the {1 0 0} plane increases abruptly from 850 °C to 900 °C. What is more fascinating to learn from Fig. 3 is that below 900 °C, the etching depth of {1 0 0} plane was higher than that of {1 1 1} plane which indicated the etching rate on the {1 0 0} plane to be faster. However, opposite case was observed when etching was completed at 950 °C. Authors are aware that the P–V values here may not guarantee the etching depths because the original surfaces of all the planes were etched away, however, the agreement between these results with the qualitative inspection of the SEM images suggest that these quantitative values here are a reliable measure for the extent of etching.

Table 1
Characteristics of the etching behaviour on different planes of diamond at different temperatures.

Etching temperature	Crystal plane of diamond	Observations
800 °C	{1 0 0}	• Etching occurred in normal direction • The outline profile of the etching zones on the {1 0 0} planes was irregular but at some corners right angles were formed • A reversed pyramidal-like etch channel consisting of four flat {1 1 1} walls was observed and the directions of its edges were parallel to the ⟨1 1 0⟩ direction (indicated in Fig. 2 (a2))
	{1 1 1}	• No obvious traces of normal etching
900 °C	{1 0 0}	• Etched severely with the loss of pristine surface, some inverted pyramidal etch pits could well be seen (indicated in Fig. 2 (b2))
	{1 1 1}	• Tangential etching was observed in edge parts
950 °C	{1 0 0}	• Same characteristics as that of at 900 °C
	{1 1 1}	• The original planes were etched away and the smooth bottom of etch pits appeared as the replication of the {1 1 1} surface The surface morphology was rough

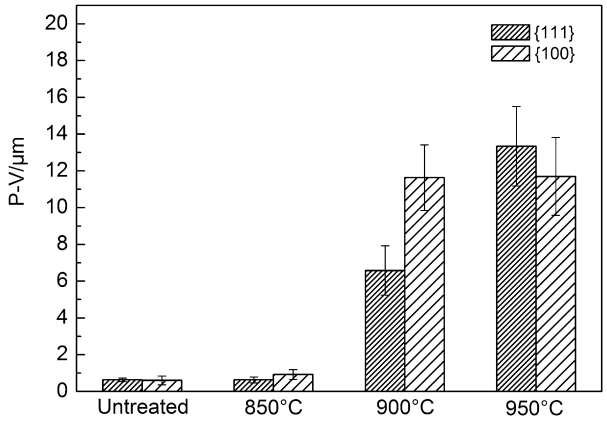

Fig. 3. The P–V values of pristine and Fe-etched diamond surface.

Table 2
Percentage of elements on the iron-loaded {1 1 1} plane treated at 900 °C analyzed by using SEM.

Element	wt%	at%
CK	53.58	78.57
OK	8.64	9.51
FeK	37.78	11.91
Matrix	Correction	ZAF

3.3. Raman spectrum of the diamond crystallites surface

The different planes of diamond before and after etching were examined by micro-Raman spectroscopy which is shown in Fig. 4. Prior to the treatment with iron powder, diamond crystallites were characterized by a sharp peak at 1330 cm^{-1} and an assumed broad sp^3 CH_2 peak around 1413 cm^{-1} [16,17]. As expected, the intensity of the sp^3 CH_2 peak on the {1 1 1} planes was stronger than that on the {1 0 0} planes. This by implication means that there were more hydrogen atoms terminating with the dangling bonds on the {1 1 1} surface of diamond. Interestingly, after being etched, there was no sp^3 CH_2 peak either on the {1 0 0} or on the {1 1 1} plane of the etched area. It was presumed that the dissociation of the hydrogen atoms from diamond surface into air was the origin of etching [18]. In fact, a graphitic carbon peak indicated by its G-band at 1578 cm^{-1} and a small D′-band at 1618 cm^{-1} [19] was identified in the severely etched area but since most of the graphite formed on the {1 1 1} surface during etching at 900 °C was etched away, only a small G-band appeared.

3.4. Element mapping and X-ray diffraction analysis

SEM image of the iron-loaded {1 1 1} plane annealed at 900 °C and the corresponding elements (C, O and Fe) mapping images are shown in Fig. 5. The carbon element (C) was observed to concentrate in the unetched part but was absent from the etching area, which indicated that the penetration depth of the X-rays into the Fe-loaded diamond sample was too shallow to detect the carbon in the iron or at the diamond–iron interface. Near the edges of the {1 1 1} plane, elemental oxygen and iron were detected which hinted towards the formation of iron oxide. The percentage of elements on the same area was analyzed and the results have been summarized in Table 2. It can be seen from Table 2 that the ratio of Fe atoms to O atoms turns out to be about 1.25 which is much larger than that 0.75 in Fe_3O_4 and 0.67 in Fe_2O_3. Based on this calculation, it can be inferred that some amount of iron was oxidized but some still existed as iron.

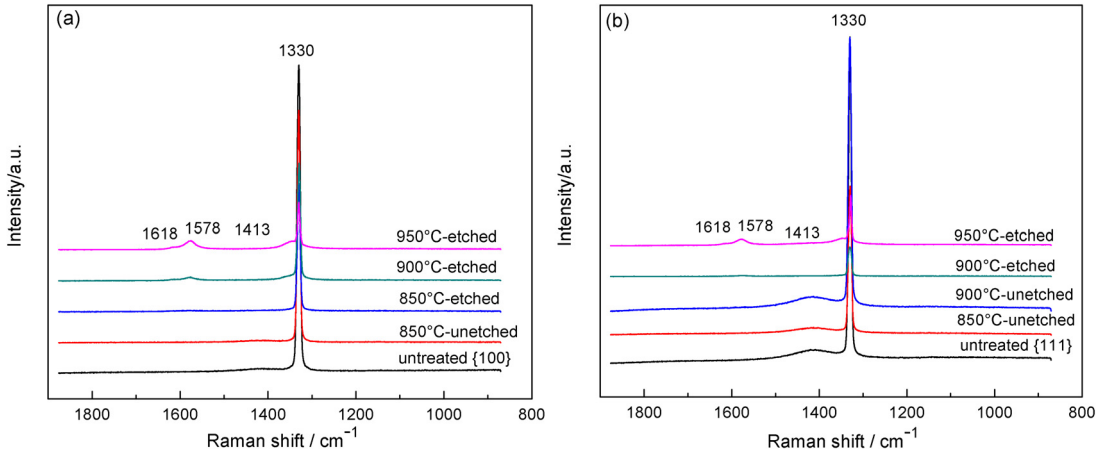

Fig. 4. Raman spectra of pristine and Fe-treated diamond: (a) {1 0 0} plane; (b) {1 1 1} plane.

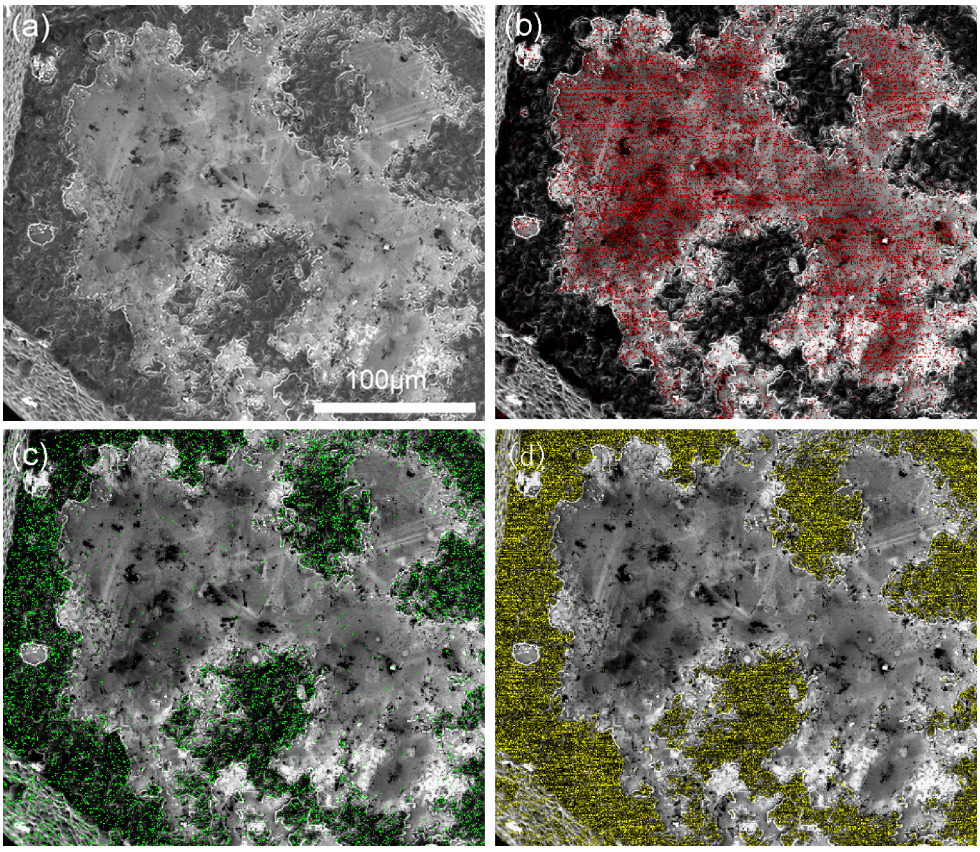

Fig. 5. Element distribution on the iron-loaded {1 1 1} plane treated at 900 °C: (a) SEM image of {1 1 1} plane, (b) carbon element mapping, (c) oxygen element mapping, (d) iron element mapping.

In order to further analyze the structure of the materials formed during etching, X-ray diffraction patterns of pristine iron powder, pristine diamond and Fe-loaded diamond annealed at 900 °C were compared in Fig. 6. From the figure, it can be seen that the pristine iron powder used in the experiment did not have any impurity of iron oxide while the as-received diamond crystallites had inclusion of iron carbide ($Fe_{2.5}C$). After the mixture of iron and diamond was annealed at 900 °C, both Fe_3O_4 and Fe were found on the diamond surface which was in accordance with the analysis shown in Table 1.

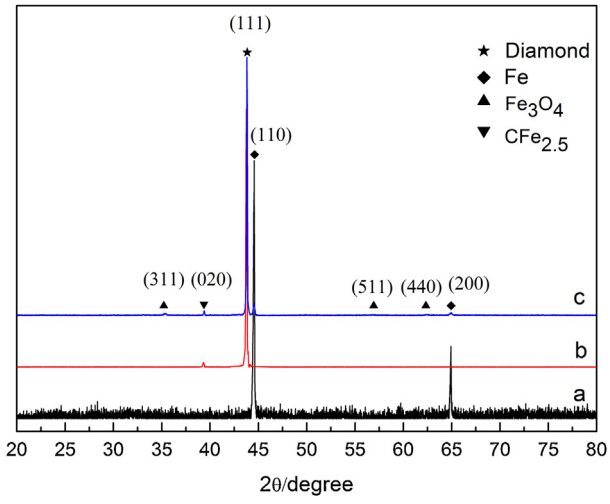

Fig. 6. X-ray diffraction pattern for (a) pristine iron powder, (b) pristine diamond and (c) Fe-etched diamond free from acid treatment.

However, it should also be noted that the peak of Fe_3O_4 was barely visible which indicated that only a small part of iron atoms were able to oxidize. This information lends credence to the argument that the graphite paper wrapped around the iron–diamond mixture can effectively prevent the oxygen in the air to enter into the reaction area. Besides, no newly formed iron carbide or graphite was found in the X-ray pattern of the Fe-loaded diamond sample. This is because of the fact that the penetration depth of X-ray beam into the diamond is too deep (about 600 μm) [20] which only allows it to detect the structural information in the volume of diamond while the composition of the sub-surface may not well be detectable. It is therefore still uncertain if there may be some iron carbide present in the iron particles or at the interface of diamond–iron.

4. Discussion

As mentioned earlier, under the same etching temperature below 900 °C, the {1 0 0} plane of diamond was easier to be normally etched than the {1 1 1} plane. This difference is attributed to the wettability and activation energy for graphitization between {1 0 0} and {1 1 1} plane. It is known that the surface energies for {1 0 0} and {1 1 1} plane of diamond are 9207 and 3387 mJ/m^2, respectively [21]. In addition, the micro-Raman spectroscopy results showed that more number of hydrogen atoms were terminated to the dangling bonds on {1 1 1} plane, which further lowered the surface energy of the plane. Therefore, it is difficult for {1 1 1} plane to get wetted by the molten iron. Even if the {1 0 0} and {1 1 1} plane become equally wetted, the {1 1 1} plane will be more stable against etching because of higher activation energy needed for graphitization [22]. Consequently, no traces of normal etching were found on {1 1 1} plane when annealed at low temperature (e.g. at

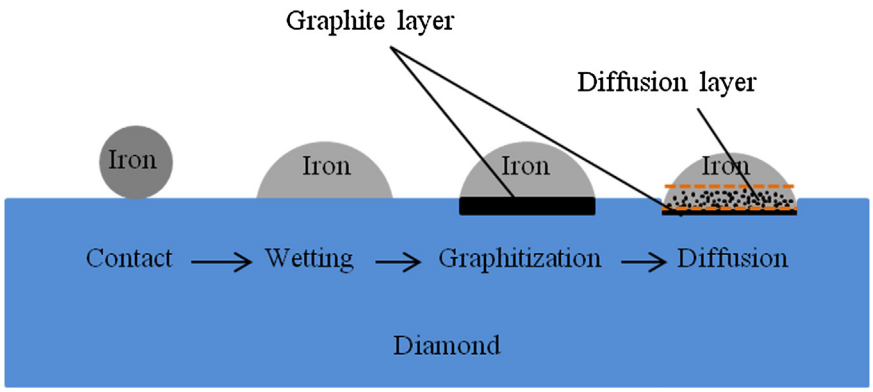

Fig. 7. Schematic model for etching diamond using iron.

850 °C and 900 °C) and also {1 1 1} plane acted as stopping planes when etch pits or channels formed on {1 0 0} plane.

Furthermore, it has been demonstrated that an increase in temperature could accelerate the etching process of diamond significantly. On one hand, higher temperature can provide more energy to convert diamond to graphite. On the other hand, an increase in temperature results in more crystal defects in iron which means more interstices are available for carbon atoms to diffuse. Thus, the solubility limit of carbon in the molten iron will be greatly improved. Especially when the temperature elevates from 850 °C to 900 °C, the structure of iron changed from bcc (α-Fe phase) to fcc (γ-Fe phase) resulting in a large change in diffusion coefficient of carbon. This is why the extent of normal etching on {1 0 0} plane increased suddenly at 900 °C. At the same time, for the {1 1 1} plane, despite the normal etching was not observed, the tangential etching did occur which implies the origin of graphitization on the {1 1 1} plane. However, tangential etching was only visible on the {1 1 1} plane. Similar to the cleavage in diamond, such a phenomenon might have become preferential on the closest packed plane with weak interlayer bond. This is a fertile area for further research.

Based on the analysis in supplemented material, it demonstrates that even if quite slight amount of iron oxide formed on diamond surface might contribute to the etching, its effect on etching should be quite small and can be ignored. Thus, graphitization of diamond is considered as the main etching mechanism here and a schematic model is proposed as shown in Fig. 7. At lower temperatures, solid iron powder establishes a mechanical contact with the surface of diamond. An increase in temperature causes gradual melt of iron particles and dissociation of hydrogen terminated on the dangling bonds. As a result, the contact condition between iron and diamond changes. Upon wetting by the molten iron, diamond tends to undergo a phase transformation from its stable sp^3 form to sp^2 when it is energetically favourable. Subsequently, the newly formed graphitic carbon at the interface of diamond and iron gets transported through the molten metal. That is to say, the graphitization of diamond and carbon diffusion in molten iron are the major mechanisms for the removal of carbon material and the formation of etch pits or channels on diamond surfaces.

5. Conclusions

In this work, an attempt has been made to etch synthetic diamond crystallites using iron powder without flowing hydrogen. Experimental results showed that at the same temperature the {1 0 0} plane was etched more rapid in comparison to the {1 1 1} plane, and that the increase in temperature accelerated the etching on both {1 0 0} and {1 1 1} plane. On the {1 0 0} plane, inverted pyramid-like pits and channels with {1 1 1} plane were formed after etching; on the {1 1 1} plane, however, edge recession and holes with flat bottoms were formed. Furthermore, the main mechanism of etching involves the transformation of diamond to graphite at the diamond–iron interface and the following diffusion of carbon in the molten iron. The etching technique proposed in this study can be used to roughen the diamond surface and increase the effective surface area of diamond, which will benefit the interfacial adhesion between diamond and bond materials.

Acknowledgements

This project has been financially supported by National Natural Science Foundation of China (Grant No. 51375157). The first author (Junsha Wang) would also like to acknowledge the China Scholarship Council (CSC) for providing her exchange scholarship for Ph.D. study and research at Keio University.

Appendix A. Supplementary data

Supplementary data associated with this article can be found, in the online version, at http://dx.doi.org/10.1016/j.apsusc.2015.04.022

References

[1] J.H. Liu, Z.J. Pei, Graham R. Fisher, Int. J. Mach. Tool Manuf. 47 (2007) 1–13.
[2] W.J. Zong, D. Li, T. Sun, K. Cheng, Y.C. Liang, Int. J. Mach. Tool Manuf. 47 (2007) 864–871.
[3] A. Tomita, Y. Tamai, J. Catal. 27 (1972) 293–300.
[4] Y. Tamai, H. Watanabe, A. Tomita, Carbon 15 (1977) 103–106.
[5] C.W. KeeP., S. Terry, M. Wells, J. Catal. 66 (1980) 451–462.
[6] P.J. Goethel, R.T. Yang, J. Catal. 114 (1988) 46–52.
[7] V.G. Ralchenko, T.V. Kononenko, S.M. Pimenov, et al., Diamond Relat. Mater. 2 (1993) 904–909.
[8] A.I. Chepurov, V.M. Sonin, J.M. Dereppe, Diamond Relat. Mater. 9 (2000) 1435–1438.
[9] V.M. Sonin, A.I. Chepurov, I.I. Fedorov, Diamond Relat. Mater. 12 (2003) 1559–1562.
[10] V.M. Sonin, Inorg. Mater. 40 (2004) 20–22.
[11] A.I. Chepurov, V.M. Sonin, P.P. Shamaev, A.P. Yelisseyev, I.I. Fedorov, Diamond Relat. Mater. 11 (2002) 1592–1596.
[12] A.I. Chepurov, V.M. Sonin, A.A. Chepurov, E.I. Zhimulev, B.P. Tolochko, V.S. Eliseev, Inorg. Mater. 47 (2011) 864–868.
[13] A.I. Chepurov, V.M. Sonin, A.A. Chepurov, E.I. Zhimulev, S.S. Kosolobov, N.V. Sobolev, Doklady Earth Sci. (2012) 1284–1287.
[14] T. Ohashi, W. Sugimoto, Y. Takasu, Appl. Surf. Sci. 258 (2012) 8128–8133.
[15] T. Ohashi, W. Sugimoto, Y. Takasu, Diamond Relat. Mater. 20 (2011) 1165–1170.
[16] M. Veres, S.T.O.T.E. Perevedentseva, A. Karmenyan, M. KoOS, Nanostruct. Mater. Adv. Technol. Appl. (2009) 115–121.
[17] M. Veres, S. Toth, M. Koos, Appl. Phys. Lett. 91 (2007) 031913.
[18] M. Uemura, Tribol. Int. 37 (2004) 887–892.
[19] L.J. Hardwick, H. Buqa, P. Novak, Solid State Ionics 177 (2006) 2801–2806.
[20] N.G. Ferreira, E. Abramof, N.F. Leite, E.J. Corat, V.J. Trava-Airoldi, J. Appl. Phys. 91 (2002) 2466–2472.
[21] M. Tsukada, S. Tsuneyuki, N. Shima, Surf. Sci. Lett. 164 (1985) L811–L818.
[22] E. Paul, C.J. Evans, A. Mangamelli, M. McGlauflin, R.S. Polvani, Precis. Eng. 18 (1996) 4–19.